Study Of Photocapacitor Transient Response Of $MAPbI_3$ Perovskite-based Solar Cell Devices

Erry Dwi Kurniawan[1*], Reni Dwi Putri[2], Widhya Budiawan[1], Shobih[1], Iqbal Syamsu[1], and Irzaman Husein[2]

[1] *Research Center for Electronics, National Research and Innovation Agency (BRIN), Bandung, West Java, Indonesia, 40135*
[2] *Department of Physics, IPB University, Bogor, Indonesia, 16680*
[*] *Corresponding author. E-mail: erry.dwi.kurniawan@brin.go.id*

Received: Aug. 04, 2025; Accepted: Oct. 23, 2025

Perovskite material ($MAPbI_3$) solar cells were used because of their capability to respond to light. The transient response characteristics of $MAPbI_3$ perovskite-based solar cell devices with and without SnO_2 layer were investigated in this paper. Under the illumination of red, green, and blue light sources, the capacitance measurement was carried out with a variation of series resistor with solar cell devices. To ensure statistical robustness, five identical devices were fabricated and tested for each configuration, and the average values were reported. $MAPbI_3$ perovskite devices with SnO_2 layer show fast responsiveness to variations in light intensity with response time (τ) reduces from 25.7 ms to 13.4 ms that is attributed to the enhanced electric field increases and accelerated accumulation charge. The peak of output voltage ($V_{\text{out,max}}$) increases in the dark condition from 0.32 V to 0.53 V , revealing that the SnO_2 layer functions as an electron transport layer with a sufficiently wide band gap to facilitate charge separation and accumulation at the electrodes. The highest output voltage of a perovskite solar cell with the SnO_2 layer occurs under the illumination of the red light source due to its low-energy photons that allow electron to be excited from valence band to conduction band, thus absorbing photons at high wavelengths. Furthermore, the capacitance (C) of devices with the SnO_2 layer decreased from 2.573μ F to 1.342μ F compared to those without the layer. These findings demonstrate that transient response characteristics enable perovskite solar cells with SnO_2 layers to function as effective photo-capacitive sensors.

Keywords: Perovskite, Photocapacitor, Solar cell, SnO_2 layer, Transient response

http://dx.doi.org/10.6180/jase.202607_30.007

1. Introduction

Metal halide perovskites are new light-absorbing materials used in photovoltaic (PV) cells for nearly a decade [1]. Rapid improvements in the power conversion efficiency of perovskite solar cells have been reported in recent years. In addition to thermoelectric generators [2, 3], solar cells can also be employed for energy harvesting, offering a sustainable solution for renewable energy applications [4]. Perovskite solar cells (PSCs) have recently achieved a high photo conversion efficiency (PCE) of $\sim$ 25% [5]. Metal halide perovskite was used because it has a sizeable photoconductive response and a dielectric constant that changes significantly under illumination [6]. In addition, the high light absorption rate in the visible to near-infrared range is one of the advantages of metal halide perovskite [7]. This is due to the Molar Extinction Coefficient (MEC) value in this material of $1.5 \times 10^4 \text{M}^{-1}\text{cm}^{-1}$ at a wavelength of 550 nm [8]. This advantage allows the material to absorb light at a layer thickness of $500 - 600$ nm, and the material is ambipolar, meaning it can conduct p-type and n-type electrical charges [7]. In addition, this material is a semiconductor with a band gap energy value of 1.55 eV [9]. The small

band gap energy value makes it easier for electrons in the material to move from the valence band to the conduction band, making it easier to conduct electricity.

One of the exciting innovation is the photocapacitor, a device that combines the functions of a solar cell and a capacitor. A photocapacitor is a capacitor that is responsive to light by converting light energy into electrical energy. A photocapacitor functions to detect responses to light stimuli [10]. The capacitor consists of two conducting plates separated by a dielectric material, while the photocapacitor uses photoconductive material as its dielectric because it is responsive to light.

In a metal halide perovskite solar cell, the tin-oxide (SnO_2) layer was added as an electron transport layer to reduce the occurrence of charge recombination. It has a light transmittance of 90%, so the applied light will pass through this material [11]. The energy band gap of $3.5-4$ eV makes this material unable to absorb visible light but can pass through it, so it is very transparent in the visible light spectrum. In addition, a reasonably wide band gap can reduce the occurrence of charge recombination so that electrons and holes remain separate so that they can produce electric current, thereby improving the performance. Apart from that, it can protect the perovskite layer from being easily degraded by environmental factors such as oxygen and humidity because the material stability of SnO_2 is relatively high.

In this study, we investigated the output voltage, capacitance, response time, current to light intensity, and the effect of adding the SnO_2 layer into perovskite solar cell devices using transient capacitor measurements. The transient response of perovskite devices has been extensively studied by measuring RC charging dynamics under the illumination of the light [12, 13]. These studies establish the role of transport layers, ion migration, and interface capacitance in defining the time constant (τ) and overall transient performances.

In this paper, we have emphasized that the novelty lies in combining the concept of a $MAPbI_3$ photocapacitor with SnO_2 integration within the RC transient measurement framework. While $MAPbI_3$ devices have been widely studied for their photoactive properties, our work uniquely demonstrates how the addition of the SnO_2 electron transport layer not only enhances the transient response by reducing the RC time constant but also improves charge accumulation and discharge dynamics. This integration provides a new perspective on tailoring perovskite-ETL interfaces for photo-capacitive applications, bridging solar cell physics with sensor functionality.

2. Materials and methods

Figure 1 shows the device structure of a perovskite solar cell with and without the SnO_2 layer. The device was made on the conductive glass FTO (fluorine tin oxide) substrate as a transparent electrode with a size of 1.5 cm $\times$ 1.5 cm and etched in hydrochloric acid (HCl) solution to form the active layer area. Then, it was cleaned by an ultrasonic cleaner in deionized water, acetone, IPA (2-propanol), and ethanol subsequently. The drying process used nitrogen spray and an oven at 80°C for 2 hours to ensure the substrate was dry from the cleaning process.

Perovskite layer deposition was accomplished in two steps, with lead(II) iodide (PbI_2) and methyl ammonium iodide (MAI) solutions prepared independently. The PbI_2 solution was made by mixing 0.24 gPbI_2 and 0.005 g KCl into 500μ L of DMF solvent, while the MAI solution was made by mixing 0.0125 g MAI into 1 mL of IPA. Then, both solutions were heated at 70°C for 3 hours until evenly mixed without crystals (MAI), and the solution was yellow (PbI_2).

Before deposition by the spin coater, the substrate was cleaned with a UV ozone cleaner for 15 minutes. After that, it was spin-coated in a glove box by dripping 70μ L of PbI_2 solution at a speed of 6000 rpm for 40 seconds. Then, the MAI solution deposition was continued at a speed of 5000 rpm for 40 seconds. Next, it was heated at 100°C for 10 minutes and continued with silver (Ag) metallization at a thickness of 100 nm using a thermal evaporator as an electrode.

A structure variation was made with the deposition of SnO_2 as the electron transport layer before the perovskite deposition. The SnO_2 solution was created by colloidal synthesis by mixing 0.3383 g of $SnCl_2 \cdot 2H_2O$ and 0.1117 g of CH_4 N_2 S into 10 mL of deionized water, stirring for 36-48 hours until bright yellow colloid. After that, a PTFE filter was used to avoid particle contamination. The deposition was performed at 3000 rpm for 30 seconds before being heated at 200°C for 30 minutes. Figure 2 shows the fabrication process of the devices without and with SnO_2 layer.

3. Results and discussion

For the material analysis, the crystallographic structure and chemical composition information was analyzed using X-ray diffraction (XRD). Crystallization measurement was carried out using X-ray diffraction (XRD) Bruker D8 Advance 3 kW with LynxEye detector and CuKα radiation source. The device was scanned using X-rays with an incident angle of 2θ at an interval of $10^\circ - 60^\circ$ with

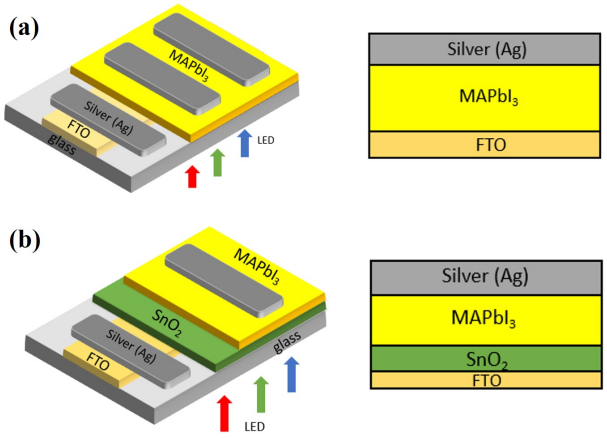

Fig. 1. Device structure with cross section (a) without SnO_2 layer (b) with SnO_2 layer.

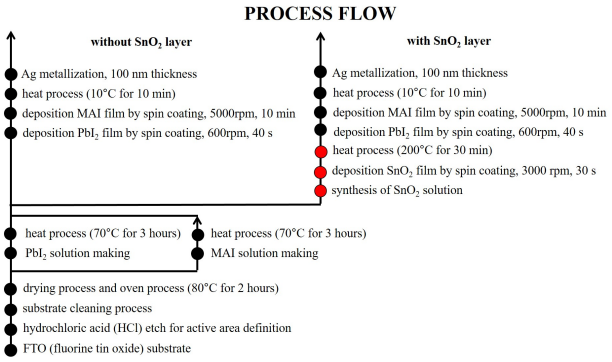

Fig. 2. Process flow of device fabrication

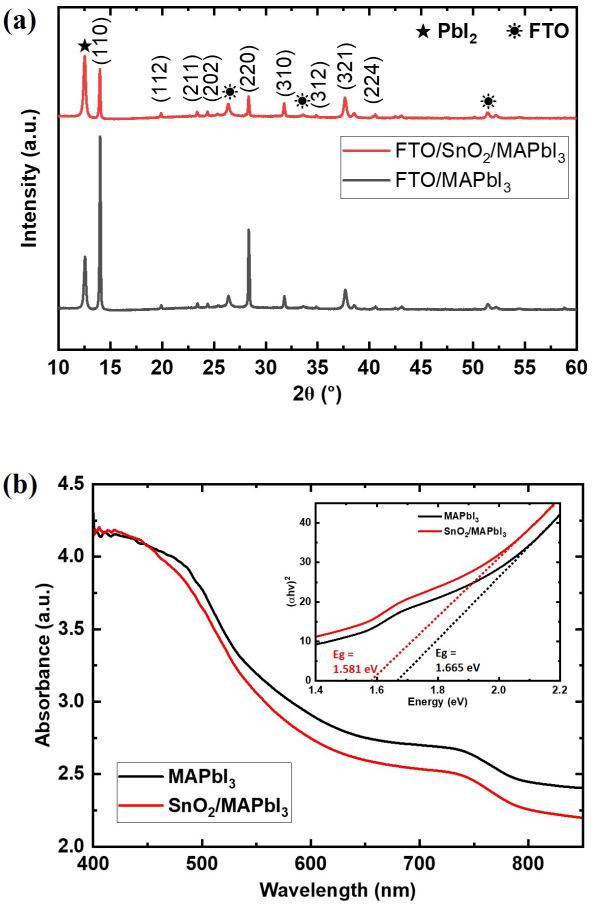

Fig. 3. (a) XRD pattern of $MAPbI_3$ devices without and with SnO_2 layer. (b) UV-Vis absorption spectra of $MAPbI_3$ devices without and with SnO_2 layer. Inset: Band gap determined using the Tauc plot method for $MAPbI_3$ devices without and with SnO_2 layer.

$\lambda = 1.54060$ Å. As shown in Figure 3(a), in the perovskite devices without the SnO_2 layer and with the SnO_2 layer, sharp peaks are produced with orientation directions (110), (112), (211), (202), (220), (310), (312), (321), and (224). Sharp and narrow peaks indicate that the material has high crystallinity and a large crystal size. A reasonably large crystal size facilitates the charge transport process and reduces the number of grain boundaries that affect charge recombination [14]. The addition of SnO_2 layers at the (110) and (220) orientations shows lower diffraction intensity peaks so that the degree of crystallinity decreases because it can attract and collect charges at the interface, thereby reducing the amount of charge for the diffraction process [15].

The optical absorption spectra were captured with a UV-Vis-NIR Maya Optic Spectrometer. To measure the spectral components of the device, the Tauc plot method used absorbance values from UV-Vis spectra by drawing an extrapolated line in the linear region of the graph relation between hv and $(\alpha hv)^2$ until it intersects the energy axis [16]. The relationship is defined as the following Equation 1:

$$(hv\alpha) = K\left(hv - E_g\right)^n \tag{1}$$

where h is Planck's constant (6.63×10^{-34}Js), v is photon frequency (c/λ), K is a proportional constant, n is $\frac{1}{2}$ for direct transition and 2 for indirect transition. The α value is the absorbance value. Perovskite materials absorb visible light in the range of $400 - 850$ nm. It can be seen in Figure 3(b) that the higher the wavelength, the lower the absorbance value because the lower the photon energy of the perovskite band gap, the more energy the photon has to excite electrons from the valence band to the conduction band. Adding a SnO_2 layer produces a lower absorbance value because the light transmission is 90%, so the applied light will pass through this material [11].

The absorbance value will affect the energy gap value.

The higher absorbance value at $(\alpha hv)^2$, the lower the absorbed photon energy, resulting in a narrower band gap value in inset picture of Figure 3(b) with the SnO_2 layer. This is following the photon energy formula (E) is given by the expression in Equation 2.

$$E = hv = hc/\lambda \tag{2}$$

where h is Planck's constant, v is the frequency of the incident light, c is the speed of light, and λ is the wavelength. The photon energy (E) is inversely proportional to the wavelength (λ). A photon can be absorbed by the perovskite layer when its energy (E) is greater than or equal to the bandgap energy ($E \geq E_g$). The absorbance value produced in this study corresponds to a tetragonal $MAPbI_3$ of $\sim$ 1.61eV at room temperature [17].

The perovskite solar cell devices were then connected in series for the transient response measurement with resistor variations of 10kΩ, 100kΩ, and 1MΩ. The function generator Agilent Keysight 33120A is used for the input voltage of 1 V with a frequency of 50 Hz . The output voltage (V_{out}) of the devices is monitored in digital oscilloscopes (Tektronix MDO3000 Series) under illumination from an LED light source (red, green, blue). The red, green, and blue LEDs used as illumination sources had intensities of 3.29 mW/cm^2, 53.27 mW/cm^2, and 75.23 mW/cm^2, respectively with emission peaks at approximately 625 nm (red), 525 nm (green), and 470 nm (blue). The measurement setup of the devices is shown in Figure 4.

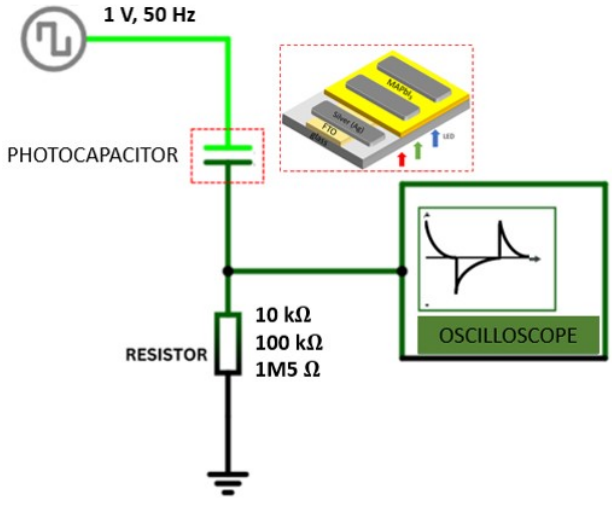

Fig. 4. The measurement setup of the devices as the RC circuit.

The perovskite solar cell devices were connected in series with a resistor with the configuration illustrated in Figure 4 to measure the capacitance in the dark condition. Figure 5 shows the graph of the transient response characteristics of the devices when charged and discharged in the dark condition for the device without SnO_2 (Figure 5(a)) and with SnO_2 (Figure 5(b)) with series resistor of 10kΩ. The charging process happens when an input voltage (V_{in}) is applied to cause charge to flow from the voltage source to the capacitor electrodes. Then, it is isolated at different distances according to the band gap of the photoactive material so that the charge accumulates on the electrodes [18].

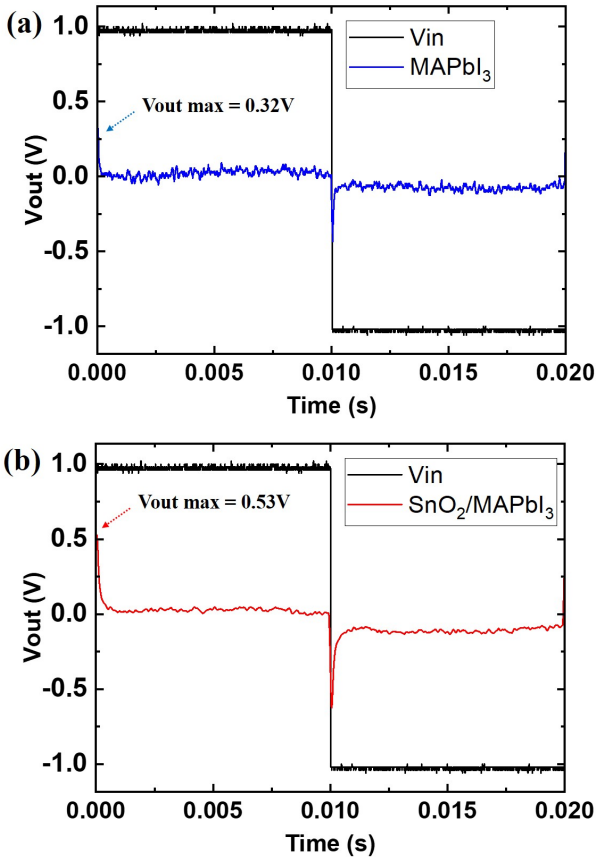

Fig. 5. The output voltage versus time of $MAPbI_3$ devices (a) without SnO_2 layer and (b) with SnO_2 layer under dark condition with a series resistor of 10 kΩ.

This charge gradually increases the output voltage following the exponential law until it approaches or equals the input voltage value of 1 volt. The exponential law for output voltage is described using the following Equation 3:

$$V = V_0\left(1 - e^{\frac{-t}{\tau}}\right) \tag{3}$$

where V is output voltage, V_0 is input voltage, e is Euler number (2.7182), t is time, and τ is time response (τ = R × C, where depend on resistor (R) and capacitance (C)).

Table 1. The extracted parameter of the perovskite devices without and with SnO_2 layer in the dark condition.

Electrical Parameters	$MAPbI_3$ Perovskite Device	
	without SnO_2 layer	with SnO_2 layer
Output Voltage, V_{out} (V)	0.32	0.53
Capacitance, C (F)	2.573×10^{-6}	1.342×10^{-6}
Current, I (A)	6.771×10^{-5}	4.736×10^{-5}
Response time, τ(ms)	25.7	13.4

The capacitance value can be extracted from Equation 3 by substituting the output voltage and time. The capacitance value is also affected by the light sensitivity response [19].

Once charged, the resistor serves as a component for current to flow from the capacitor during the discharge process. Because the positive electrode receives electrons, the chargecarrying current flows from the negative electrode to the positive, neutralizing the charge. This demonstrates that when the quantity of stored charge diminishes, the voltage reduces exponentially over time, as shown in Equation 3.

Table 1 shows the extracted parameter from the graph in Figure 5. Adding the SnO_2 layer increases the peak output voltage and current because it acts as an electron transport to separate the electric charges of electrons and holes in the photoactive layer towards the electrode to reduce recombination [8, 15]. The peak output voltages of 0.32 V and 0.53 V were obtained for devices without and with SnO_2 layers, respectively. Charge recombination occurs when electrons and holes recombine into neutral charge carriers. The response time (τ) will also decrease by reducing the recombination. This is due to the wide band gap of $3.5 - 4$eV in SnO_2. The wide band gap can separate the electric charge on each electrode so that the charge will remain stored. The output voltage and current will increase in accordance with Ohm's law ($V = I \times R$), where the voltage is directly proportional to the current. The higher output voltage will decrease the capacitance value. This is because adding electron transport material can increase the layer thickness on the photocapacitor. According to the parallel plate capacitance formula, the capacitance value (C) is directly proportional to the permittivity of the material (ε) and the capacitor plate area (A), as shown in Equation 4. However, it is inversely proportional to the distance between the plates (d). If the thickness of the layer material increases, the capacitance value will decrease.

$$C = \varepsilon \frac{A}{d} \tag{4}$$

Figure 6 shows the transient response characteristics of devices with different series resistors of $10k\Omega, 100k\Omega$, and $1M\Omega$. Using a smaller resistor of $10k\Omega$, we found that the perovskite device series leads to a rapid charging and discharging time. In contrast, the higher resistor will result in a relatively lagging charging and discharging time. This corresponds to the time response formula ($\tau = R \times C$), in which the response time is directly proportional to the resistor. The higher the resistor value will give the slower the response time.

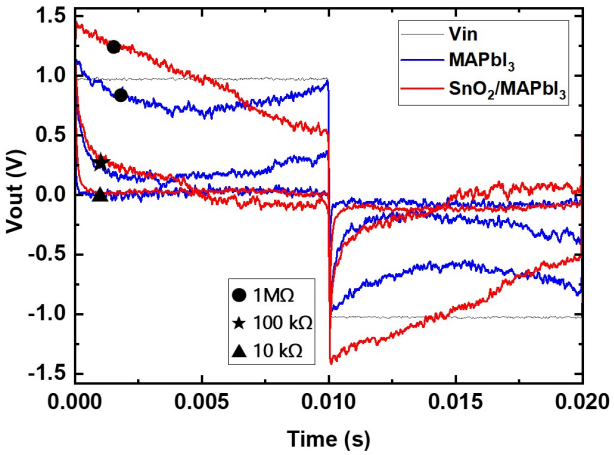

Fig. 6. The transient response characteristics of the devices with variation of series resistor of $10k\Omega, 100k\Omega$, and $1M\Omega$.

Table 2. The comparison of the output voltage of the perovskite devices without and with SnO_2 layer in the dark condition and under illumination of red, green, blue light.

Light Source	Max Output Voltage (V)	
	without SnO_2 layer	with SnO_2 layer
Red	0.55	0.81
Green	0.50	0.72
Blue	0.45	0.71
Dark	0.32	0.53

Figure 7 reveals the effect of the difference in light source wavelength illuminated into the device series with a $10k\Omega$ resistor. The output voltage of the perovskite devices without and with SnO_2 layer in the dark condition and under illumination of red, green, blue light then extracted into Table 2. The red light source generates the highest maximum output voltage due to the low-energy photons. It is

Table 3. The summary parameter of the perovskite devices without and with SnO_2 layer as the light intensity variations with resistor series of 1MΩ.

Electrical parameters	Light Intensity (I)							
	without SnO_2	with SnO_2	without SnO_2	with SnO_2	without SnO_2	with SnO_2	without SnO_2	with SnO_2
	$I = 0 Wm^{-2}$		$I = 3.29 Wm^{-2}$		$I = 53.27 Wm^{-2}$		$I = 75.23 Wm^{-2}$	
V_{max} (V)	0.207	0.834	0.431	1.177	0.982	1.680	1.474	1.702
I (μA)	34.391	11.131	34.264	8.680	9.860	6.872	7.473	6.830
τ(ms)	0.051	0.016	0.050	0.012	0.014	0.010	0.011	0.009

easier for electrons to be excited from the valence band to the conduction band in perovskite material. It can absorb photons at high wavelengths where the photon energy is inversely proportional to wavelength.

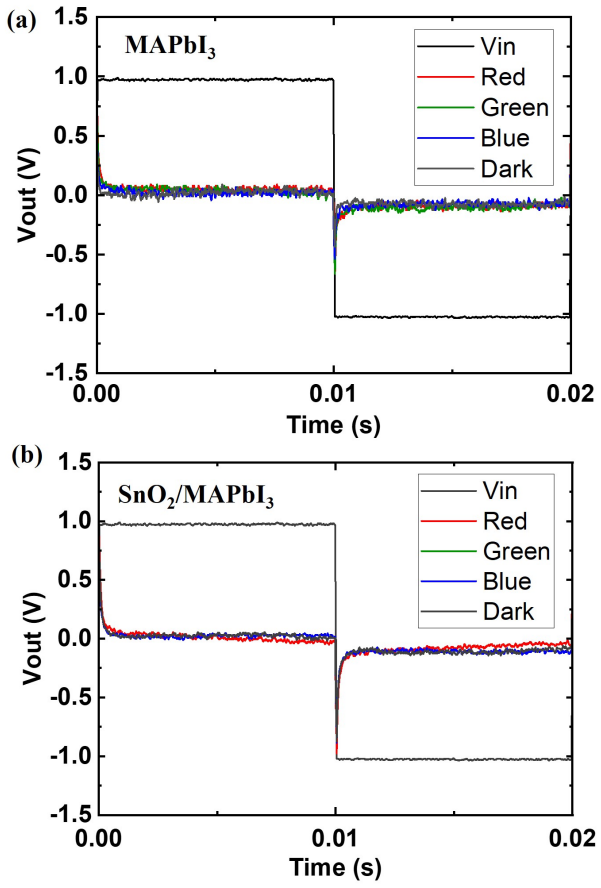

Fig. 7. The effect of light source variation (red, green, blue) on the output voltage with resistor 10kΩ.

Figure 7 depicts the output voltage and capacitance values as the function of the series resistor with the variation of the light intensity for the devices without SnO_2 and with SnO_2 layer. The higher light intensity results in the highest maximum output voltage and smaller capacitance values. Table 3 shows that the current is dropped when the voltage reaches the maximum. The response time is faster when the light intensity increases. The capacitance value is the highest in the dark condition ($0 Wm^{-2}$) because the devices absorb no photon energy. There is no addition of electron-hole pairs (neutral charge). However, the changes in light intensity reduce the capacitance value because the light carries photon energy and generates electron-hole pairs (neutral charge) [20, 21].

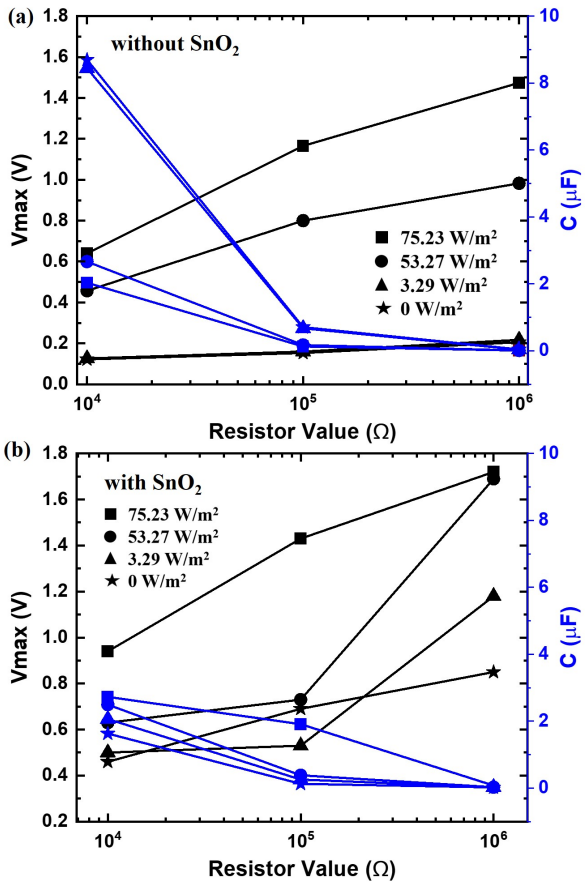

Fig. 8. The output voltage and capacitance value as the function of series resistor with the variation of the light intensity for the devices without SnO_2 layer and with SnO_2 layer.

4. Conclusions

In this paper, the transient response of $MAPbI_3$ and added SnO_2 perovskite-based solar cell device characteristics was investigated. $MAPbI_3$ perovskite film with SnO_2 layer shows responsiveness to light intensity with a fast response time. The higher light intensity results in lower capacitance values. The capacitance value is inversely proportional to the light sensitivity response. If the light intensity increases, the response time will decrease. Thus, the transient response characteristics of the devices can enable the perovskite solar cells as the photocapacitive sensor that is responsive to the changing of light.

Acknowledgements

The authors thank the Research Organization for Electronics and Informatics, National Research and Innovation Agency (BRIN) for their financial support. This research was conducted at the Science and Technology Park Prof. Samaun Samadikun, BRIN Bandung. The authors acknowledge the facilities and technical support from the laboratory of the Research Center for Electronics, National Research and Innovation Agency through E-Layanan Sains.

References

[1] P. Basumatary and P. Agarwal, (2020) *"Photocurrent transient measurements in MAPbI3 thin films"* **Journal of Materials Science: Materials in Electronics *31***(13): 10047–10054. DOI: 10.1007/s10854-020-03549-7.

[2] E. J. Majeed and A. J. Majeed, (2022) *"Harvesting Human Being Energy to Charge Smartphone"* **Jordan Journal of Mechanical and Industrial Engineering *16***(3): 439–448.

[3] E. J. Majeed and A. J. Majeed, (2024) *"Harvesting Human Energy to Power Head Torches Using a Thermoelectric Generator"* **Engineering Proceedings *70***(1): DOI: 10.3390/engproc2024070030.

[4] A. J. Majeed, (2023) *"Numerical Study for the First Phase of the Miraah Solar Well Plant in Oman"* **Procedia Structural Integrity *47***: 919–931. DOI: 10.1016/j.prostr.2023.07.023.

[5] M. A. Green, Y. Hishikawa, E. D. Dunlop, D. H. Levi, J. Hohl-Ebinger, and A. W. Ho-Baillie, (2018) *"Solar cell efficiency tables (version 52)"* **Progress in Photovoltaics: Research and Applications *26***(7): 427–436. DOI: 10.1002/pip.3040.

[6] J. G. Labram, E. E. Perry, N. R. Venkatesan, and M. L. Chabinyc, (2018) *"Steady-state microwave conductivity reveals mobility-lifetime product in methylammonium lead iodide"* **Applied Physics Letters *113***(15): 153902. DOI: 10.1063/1.5041959.

[7] M. Assadi, S. Bakhoda, R. Saidur, and H. Hanaei, (2018) *"Recent progress in perovskite solar cells"* **Renewable and Sustainable Energy Reviews *81***: 2812–2822. DOI: 10.1016/j.rser.2017.06.088.

[8] H.-S. Kim, J.-W. Lee, N. Yantara, P. P. Boix, S. A. Kulkarni, S. Mhaisalkar, M. Grätzel, and N.-G. Park, (2013) *"High Efficiency Solid-State Sensitized Solar Cell-Based on Submicrometer Rutile TiO2 Nanorod and CH3NH3PbI3 Perovskite Sensitizer"* **Nano Lett. *13***(6): 2412–2417. DOI: 10.1021/nl400286w.

[9] G. E. Eperon, S. D. Stranks, C. Menelaou, M. B. Johnston, L. M. Herz, and H. J. Snaith, (2014) *"Formamidinium lead trihalide: a broadly tunable perovskite for efficient planar heterojunction solar cells"* **Energy Environ. Sci. *7***(3): 982–988. DOI: 10.1039/C3EE43822H.

[10] C. Trujillo Herrera and J. G. Labram, (2020) *"A perovskite retinomorphic sensor"* **Appl. Phys. Lett. *117***(23): 233501. DOI: 10.1063/5.0030097.

[11] L. Xiong, Y. Guo, J. Wen, H. Liu, G. Yang, P. Qin, and G. Fang, (2018) *"Review on the Application of SnO2 in Perovskite Solar Cells"* **Advanced Functional Materials *28***(35): 1802757. DOI: 10.1002/adfm.201802757.

[12] S. Wheeler, D. Bryant, J. Troughton, T. Kirchartz, T. Watson, J. Nelson, and J. R. Durrant, (2017) *"Transient Optoelectronic Analysis of the Impact of Material Energetics and Recombination Kinetics on the Open-Circuit Voltage of Hybrid Perovskite Solar Cells"* **J. Phys. Chem. C *121***(25): 13496–13506. DOI: 10.1021/acs.jpcc.7b02411.

[13] S. Ravishankar, Z. Liu, U. Rau, and T. Kirchartz, (2022) *"Multilayer Capacitances: How Selective Contacts Affect Capacitance Measurements of Perovskite Solar Cells"* **PRX Energy *1***(1): 013003. DOI: 10.1103/PRXEnergy.1.013003.

[14] S. Morab, M. M. Sundaram, and A. Pivrikas, (2023) *"Review on Charge Carrier Transport in Inorganic and Organic Semiconductors"* **Coatings *13***(9): DOI: 10.3390/coatings13091657.

[15] P. Wu, S. Wang, X. Li, and F. Zhang, (2021) *"Advances in SnO2-based perovskite solar cells: from preparation to photovoltaic applications"* **J. Mater. Chem. A *9***(35): 19554–19588. DOI: 10.1039/D1TA04130D.

[16] K. Wang, P. Zeng, J. Zhai, and Q. Liu, (2013) *"Electrochromic films with a stacked structure of WO3 nanosheets"* **Electrochemistry Communications *26***: 5–9. DOI: 10.1016/j.elecom.2012.09.037.

[17] Y. Yamada, T. Nakamura, M. Endo, A. Wakamiya, and Y. Kanemitsu, (2014) *"Near-band-edge optical responses of solution-processed organic–inorganic hybrid perovskite CH3NH3PbI3 on mesoporous TiO2 electrodes"* **Applied Physics Express 7**(3): 032302. DOI: 10.7567/APEX.7.032302.

[18] C. Li, Z. Zang, C. Han, Z. Hu, X. Tang, J. Du, Y. Leng, and K. Sun, (2017) *"Highly compact CsPbBr3 perovskite thin films decorated by ZnO nanoparticles for enhanced random lasing"* **Nano Energy *40***: 195–202. DOI: 10.1016/j.nanoen.2017.08.013.

[19] R. Zhang, R. Li, Y. Chen, and Y. Cui, (2025) *"Ultra sensitive low-frequency visible light dielectric response measured by real capacitance method"* **Communications Materials *6***(1): 48. DOI: 10.1038/s43246-025-00771-w.

[20] D. Gonçalves, L. M. Fernandes, P. Louro, M. Vieira, and A. Fantoni. "Measurement of Photo Capacitance in Amorphous Silicon Photodiodes". In: *Technological Innovation for the Internet of Things*. Ed. by L. M. Camarinha-Matos, S. Tomic, and P. Graça. Berlin, Heidelberg: Springer Berlin Heidelberg, 2013, 547–554.

[21] C. Trujillo Herrera and J. G. Labram, (2021) *"Quantifying the performance of perovskite retinomorphic sensors"* **J. Phys. D: Appl. Phys. *54***(47): 475110. DOI: 10.1088/1361-6463/ac1d10.